ARE YOU AWARE OF HIDDEN INSTABILITIES IN YOUR RORB MODEL?

Yanni Wang[1], Tim Rhodes[1], Tim Hammond[1]

[1]SMEC, Melbourne, VIC

Abstract

RORB is widely used for rainfall–runoff modelling, yet modern high-resolution applications can introduce a hidden numerical instability at the reach scale. When the computational timestep is large relative to the effective travel time, the Crank–Nicolson routing scheme produces oscillatory artefacts that are not visible in standard model outputs.

A mathematical analysis demonstrates that this behaviour arises from the model formulation itself. Under unsteady flow, truncation errors are continuously introduced and may persist, leading to peak-flow underestimation, hydrograph distortion, and volume inconsistencies.

Two case studies illustrate the practical implications. In an extreme hydrology application, coarse timesteps suppress peak flows by up to 15% and alter critical storm duration. Across 30 urban catchments, 20–40% of reaches exhibit mass-balance discrepancies, with peak-flow underestimation of up to 8–11% in affected reaches and systematic distortion of temporal patterns.

A hydrological Courant number is proposed to relate timestep, reach length, calibration parameter, and flow magnitude. This provides a practical diagnostic tool for assessing timestep adequacy and identifying conditions under which instability may occur.

These findings demonstrate that timestep selection and model discretisation are not purely numerical choices, but key modelling decisions. Without appropriate alignment between timestep and system response, routing instability can remain undetected while materially influencing flood estimates and downstream hydraulic modelling outcomes.

1. Introduction: hidden instability in RORB

RORB is widely used for rainfall–runoff modelling in Australia and forms a key component of many flood estimation workflows. While the model has been applied for several decades with a largely unchanged routing formulation, contemporary practice has evolved significantly, with increasing spatial resolution and broader use of routed hydrographs in downstream hydraulic modelling.

To examine the numerical behaviour underlying this formulation, a synthetic catchment was constructed (Figure 1), consisting of uniform subareas of 1 km^2 and reach lengths of 1 km. The model was run under steady rainfall with the same routing parameters and zero losses to isolate routing behaviour.

Figure 1 presents four cases of the simulated hydrograph at the outlet and along Reach R3, representing different combinations of timestep and flow magnitude. In all cases, rainfall input and model parameters are identical, and the system is expected to approach a steady-state discharge. Despite this, the simulated hydrographs exhibit markedly different behaviour.

For small timesteps relative to the catchment response time (Cases 1a and 1c), the solution generally converges towards equilibrium. In Case 1a, the response is smooth and monotonic. In Case 1c, however, a small oscillation is evident during the initial timesteps due to the higher inflow. This oscillation decays rapidly and becomes negligible after a few timesteps.

In contrast, when the timestep is large (Cases 1b and 1d), the solution exhibits sustained oscillatory behaviour, with alternating overshoot and undershoot around the steady-state discharge. The effect is more pronounced at higher flows. In Case 1d, the oscillations decay so slowly that they persist over the duration of the simulation, despite the system being theoretically stable.

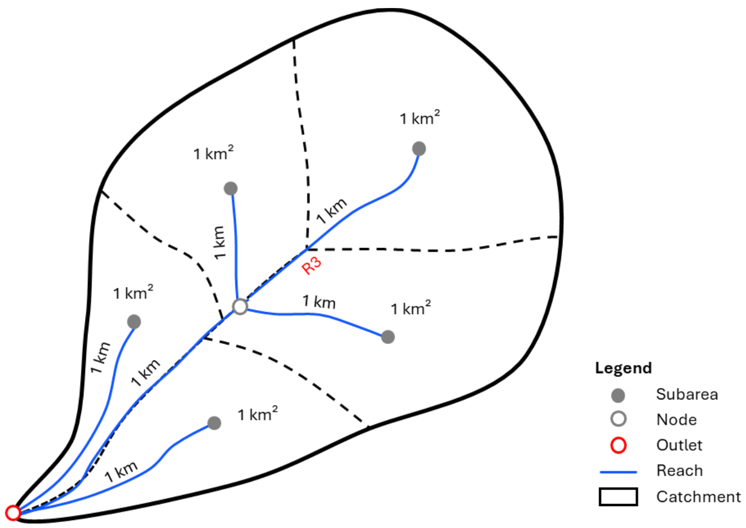

Figure 1 Synthetic catchment layout of case 1

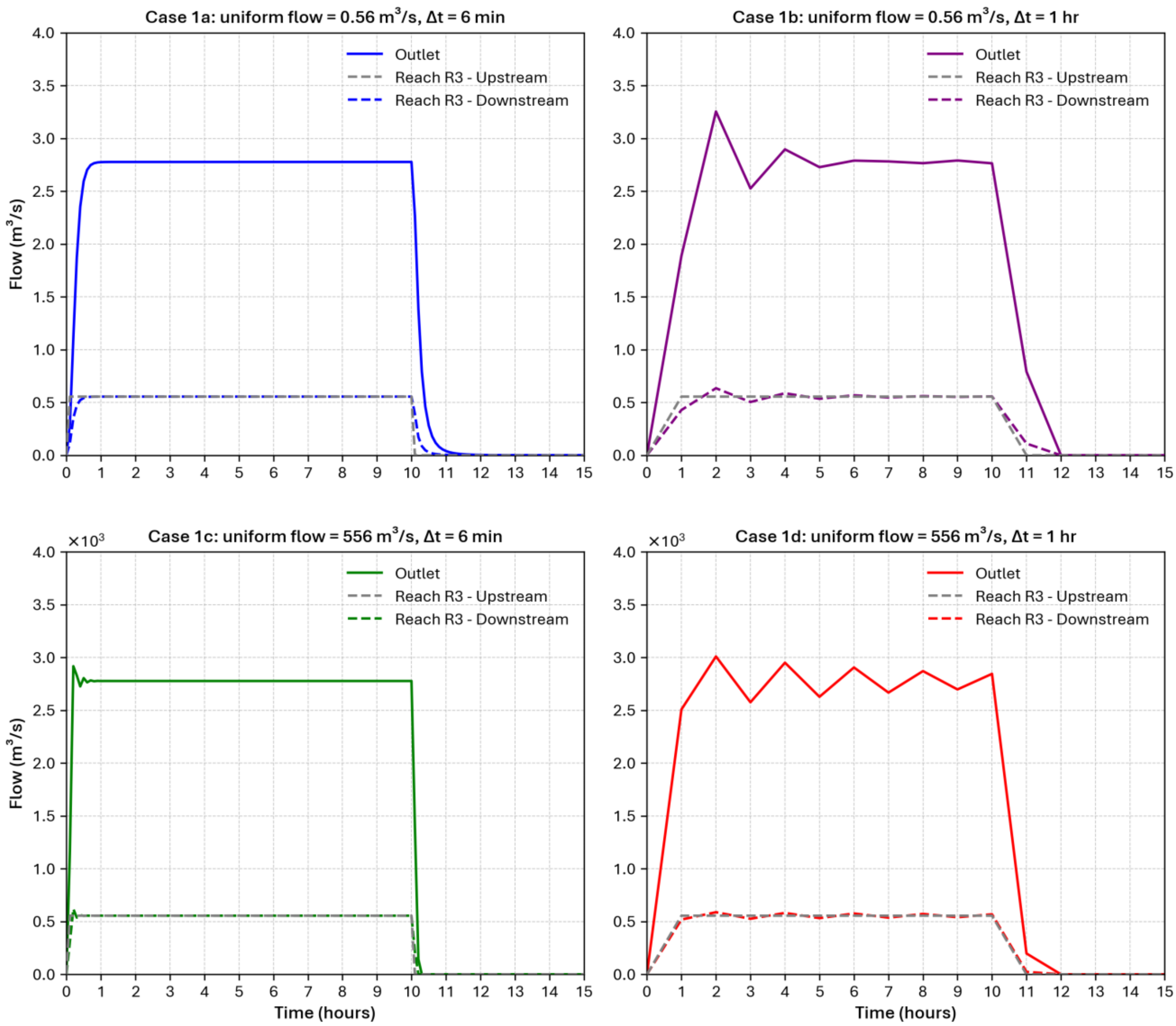

Figure 2 Comparison of hydrographs at catchment outlet and Reach R3 under different combinations of timestep and flow magnitude

These results demonstrate that the numerical behaviour of RORB routing depends not only on model parameters and rainfall forcing, but also on the relationship between timestep and the effective response time of the storage element. Importantly, the oscillatory behaviour is not caused by failure of the solution algorithm, but arises from the time discretisation used in the routing scheme.

In practical applications, this behaviour can remain undetected. A model may produce a smooth hydrograph at the outlet and calibrate well against observed data, while internal reaches experience oscillatory artefacts that influence peak flow, timing, and volume consistency. This issue becomes more relevant as catchment discretisation increases, leading to shorter reaches and reduced travel times, which increase sensitivity to timestep selection.

Despite its potential impact, this behaviour has received limited attention in standard modelling practice. There is currently no direct diagnostic within RORB to identify reach-scale instability, and the interaction between timestep, reach length, and flow magnitude is not commonly evaluated.

This paper investigates the origin, behaviour, and practical implications of this instability. A mathematical analysis is first presented to explain the oscillatory behaviour arising from the Crank–Nicolson discretisation of the storage equation. The implications are then demonstrated through case studies representing extreme hydrology and urban flood modelling applications. Finally, a hydrological Courant condition is introduced to provide a practical framework for diagnosing instability, together with recommendations for model setup and application.

2. Oscillatory numerical artefacts in RORB routing

2.1 Mathematical explanation

RORB storage–discharge formulation

RORB represents catchment storage using the nonlinear storage–discharge relationship (RORB Manual, 2010):

$$S = 3600kQ^m \tag{1}$$

where S is catchment storage (m^3), Q is outflow (m^3/s), k is the storage coefficient (hours), and m is the nonlinearity exponent. The factor 3600 converts k from hours to seconds.

The water balance for each timestep is given by:

$$\frac{\Delta S}{\Delta t} = I - Q \tag{2}$$

where I is inflow (m^3/s).

RORB applies a Crank–Nicolson (CN) trapezoidal discretisation to both sides, averaging inflow and outflow across the timestep (RORB Manual, 2010):

$$3600k\frac{{Q_{t+1}}^m - {Q_t}^m}{\Delta t} = \frac{I_t + I_{t+1}}{2} - \frac{Q_t + Q_{t+1}}{2} \tag{3}$$

Rearranged form solved by the root-finder

Multiplying Equation (3) through by Δt and collecting all Q_{t+1} terms on the left gives:

$$3600kQ_{t+1}^m + \frac{\Delta t}{2}Q_{t+1} = 3600kQ_t^m - \frac{\Delta t}{2}Q_t + I_{avg}\Delta t \tag{4}$$

where $I_{avg} = (I_t + I_{t+1})/2$.

Equation (4) implicitly defines a timestep mapping:

$$Q_{t+1} = g(Q_t, I_t, I_{t+1}) \tag{5}$$

which must be solved numerically at each timestep.

Define:

$$h(Q) = 3600kQ^m + \frac{\Delta t}{2}Q \tag{6}$$

so that the root-finder solves:

$$h(Q_{t+1}) = \text{RHS} \tag{7}$$

The derivative of h is:

$$h'(Q_{t+1}) = 3600kmQ_{t+1}^{m-1} + \frac{\Delta t}{2} > 0 \tag{8}$$

which shows that $h(Q)$ is strictly increasing.

Therefore Equation (4) has a unique solution, and any bracketing root-finding method (e.g. Regula Falsi, bisection or secant) will converge to that solution. The oscillatory behaviour observed in RORB simulations is therefore not caused by failure of the root-finding algorithm, but by the properties of the time discretisation itself.

Amplification factor

The behaviour of the time-stepping scheme can be analysed using the amplification factor, defined as the Jacobian of the timestep mapping evaluated at steady state:

$$r = \left.\frac{dg}{dQ_t}\right|_{Q^*} \tag{9}$$

Implicit differentiation of:

$$h(Q_{t+1}) = \text{RHS}(Q_t) \tag{10}$$

with respect to Q_t gives

$$\left(3600kmQ_{t+1}{}^{m-1} + \frac{\Delta t}{2}\right)\frac{dQ_{t+1}}{dQ_t} = 3600kmQ_t{}^{m-1} - \frac{\Delta t}{2} \tag{11}$$

Define the storage inertia:

$$\lambda_t = \frac{dS}{dQ} = 3600kmQ_t{}^{m-1} \tag{12}$$

The parameter λ therefore represents the characteristic response time of the nonlinear storage element.

Substituting into Equation (11), then the amplification factor is:

$$r_{CN} = \frac{\lambda_t - \Delta t/2}{\lambda_{t+1} + \Delta t/2} \tag{13}$$

The denominator of Equation (13) is equal to $h'(Q_{t+1})$ from Equation (8), confirming consistency between the two formulations.

Evolution of perturbations

The amplification factor r describes how numerical errors propagate between timesteps. Consider a small perturbation ε_t at timestep t. The perturbation evolves approximately as:

$$\varepsilon_{t+1} \approx r\varepsilon_t \tag{15}$$

In general, $|\, r \,| > 1$ would imply amplification of perturbations. However, for the CN discretisation of the RORB storage equation, $|\, r \,| < 1$ always. The practical issue is therefore not divergence, but the occurrence of oscillatory decay when $r < 0$. In this case the perturbation changes sign at each timestep, producing alternating overshoots about the equilibrium. As $r \to -1$, these oscillations decay very slowly and may persist for many timesteps.

Since the denominator of Equation (13) is always positive, the sign of r is determined by the numerator and therefore depends on the relationship between λ and the timestep Δt. This determines the type of convergence:

- $r > 0$ when $\lambda > \frac{\Delta t}{2}$, i.e. $\Delta t < 2\lambda$ – monotone convergence
- $r < 0$ when $\lambda < \frac{\Delta t}{2}$, i.e. $\Delta t > 2\lambda$ – oscillatory convergence

Flow-dependent behaviour

For $m < 1$, the exponent $m - 1 < 0$, so storage inertia decreases as flow increases:

$$\lambda \propto Q^{m-1} \tag{16}$$

The oscillation threshold 2λ therefore becomes smaller at higher flows. Consequently, even a relatively small timestep can enter the oscillatory regime at large discharges.

The sign change in the numerator of Equation (13) occurs when:

$$Q_{crit} = \left(\frac{\Delta t}{2 \times 3600km}\right)^{\frac{1}{m-1}} \tag{17}$$

For $Q > Q_{crit}$, the amplification factor becomes negative, and the scheme produces oscillatory decay.

Decay rate

When $r < 0$, oscillations decay geometrically. If the initial deviation is ε_0, then after n steps:

$$|\varepsilon_n| = |\varepsilon_0||r|^n \tag{18}$$

Since geometric decay never reaches zero exactly, damping can be defined as the time required for the oscillation amplitude to fall below a threshold τ:

$$|\ \varepsilon_0\ |\cdot|\ r\ |^n < \tau \tag{19}$$

Solving for n gives:

$$n > \frac{\ln(\tau/|\varepsilon_0|)}{\ln(|r|)} \tag{20}$$

The corresponding simulated time is $n \times \Delta t$.

Plain-English summary

The parameter:

$$\lambda = 3600kmQ^{m-1}$$

represents the storage inertia of the catchment, or how quickly outflow responds to changes in inflow. Large λ corresponds to a slow, buffered response, while small λ represents a rapid, flashy system.

The numerical behaviour depends on how the timestep compares to this response time. When the timestep is small relative to λ, the solution evolves smoothly. When the timestep is large, the scheme alternates around the equilibrium, producing oscillations.

The amplification factor r controls how long this oscillation persists. Values close to one lead to slowly decaying oscillations that can remain visible throughout the hydrograph.

An intuitive analogy is parking a car in a tight space. If your reaction time is short relative to how far the car moves between corrections, you can steer smoothly into position. If your reaction time is long, the car repeatedly passes the desired position and must be corrected back and forth before settling.

The CN scheme behaves in a similar way. At each timestep it estimates the new discharge. When the timestep is too large relative to the catchment response, each update overshoots the equilibrium and the solution alternates around it.

2.2 Numeric demonstration

The flow behaviour observed in Figure 1 can be explained using the mathematics presented above. Table 1 summarises the amplification factor r, critical flow and decay rate of Reach R3 for the four synthetic cases.

Case 1a is the only case with $r > 0$, and therefore the only case representing monotonic which represents physically storage filling. When $r < 0$, the solution becomes oscillatory, and the magnitude of r controls the rate of decay. Cases with $|\ r\ |$ well below 1 (e.g. Case 1c) exhibit rapidly damped oscillations, whereas cases where $r$approaches -1(e.g. Case 1d) decay very slowly, with oscillations persisting over many timesteps.

The critical flow provides a clear interpretation of the transition between these regimes. For the 6-minute timestep, the critical flow is approximately 32 m^3/s. Case 1a remains below this threshold and therefore converges monotonically, whereas Case 1c exceeds it and becomes oscillatory despite using the same timestep. For the 1-hour timestep, the critical flow reduces to approximately 32×10^{-4} m^3/s, meaning both Cases 1b and 1d fall within the oscillatory regime.

Table 1 Summary of amplification factor and decay characteristics for the four synthetic cases

Case	Condition		Amplification			Critical flow	Decay below 1% of flow	
	Δt (s)	Q^* (m^3/s)	λ^* (s)	r value	Behaviour	Q_{crit} (m^3/s)	n steps	Duration
1a	360	0.56	648	+0.57	Monotone	336	N/A	N/A
1b	3600	0.56	648	−0.47	Oscillatory	3.36×10^{-3}	6	6 hr
1c	360	556	163	−0.05	Oscillatory	336	2	12 min
1d	3600	556	163	−0.83	Oscillatory	3.36×10^{-3}	25	25 hr

2.3 Mechanisms producing oscillatory artefacts under unsteady flow

The steady-state analysis showed that the amplification factor r determines whether perturbations decay monotonically or oscillate while decaying, and how rapidly they diminish. The decay rate is controlled by the magnitude $|\, r \,|$.

In a real hydrograph, however, the flow Q evolves continuously, which in turn changes the storage inertia λ and the amplification factor. Consequently, the numerical behaviour of the scheme is no longer governed by a single constant r; both the oscillatory tendency and the rate of damping can vary throughout the event.

Continuous seeding of perturbations

Under unsteady inflow, a new perturbation is introduced at every timestep:

$$\varepsilon_{t+1} = r_t \varepsilon_t + \delta_t \tag{21}$$

where r_t is the local amplification factor and δ_t is the perturbation introduced by the changing inflow.

The CN scheme uses the average inflow

$$I_{avg} = \frac{I_t + I_{t+1}}{2} \tag{22}$$

instead of the end-of-step inflow I_{t+1}. Compared with a fully implicit scheme that uses I_{t+1}, this introduces a systematic truncation error proportional to $\Delta I_t/2$ in the right-hand side of Equation (4), where:

$$\Delta I_t = I_{t+1} - I_t \tag{23}$$

The resulting discharge perturbation is:

$$\delta_t = -\frac{\Delta I_t/2}{h'(Q_{t+1})} = -\frac{\Delta t \cdot \Delta I_t/2}{\lambda_{t+1} + \Delta t/2} \tag{24}$$

During the rising limb ($\Delta I_t > 0$): CN underestimates inflow, producing $\delta_t < 0$. During the falling limb ($\Delta I_t < 0$): CN overestimates inflow, producing $\delta_t > 0$.

These truncation errors are small when the scheme is monotone. However, when $r < 0$, each perturbation generates a sequence of alternating-sign errors, producing a jagged hydrograph.

Error accumulation

Expanding the recursion over N steps from an initial zero error gives:

$$\varepsilon_N = \sum_{t=0}^{N-1} \left(\prod_{j=t+1}^{N-1} r_j \right) \delta_t \tag{25}$$

Each perturbation δ_t introduced at timestep t is multiplied by the product of all subsequent amplification factors. The influence of past perturbations therefore depends on how strongly the numerical scheme transmits errors between timesteps.

Under unsteady flow, inflow varies from one timestep to the next, so new perturbations δ_t are continuously introduced. When $|\, r_t \,|$ is close to one, these perturbations decay only slowly, allowing oscillations to persist and accumulate in the simulated hydrograph.

Unpredictable sign of peak-flow error

During the steep rising limb, $\delta_t < 0$ at every step. Because $r < 0$, each perturbation alternates sign at subsequent timesteps. The peak-flow error can therefore be approximated as

$$\varepsilon_{peak} \approx r \cdot \varepsilon_{prev} + \delta_{prev} \tag{26}$$

The sign of the accumulated error depends on the number of rising-limb timesteps before the peak. Consequently, the sign of the peak discharge error can depend sensitively on the timestep and the precise timing of the peak relative to the timestep.

Bias in volume conservation

For $m < 1$, the storage function $S = 3600kQ^m$ is concave. If discharge oscillates symmetrically about Q^*, the mean storage becomes:

$$\bar{S} = \frac{S(Q^* + A_{osc}) + S(Q^* - A_{osc})}{2} \tag{27}$$

Concavity implies:

$$\bar{S} < S(Q^*) \tag{28}$$

Therefore, oscillations bias the simulated storage slightly low. The magnitude of this bias scales approximately with $(A_{osc}/Q^*)^2$. Although typically small, it alters the effective storage–discharge during oscillatory periods.

3. Case studies on how instability can alter design hydrology

This section presents two case studies illustrating how routing instability can alter design hydrology.

The percentage difference in peak discharge is defined as:

$$\frac{\left(Q_{original} - Q_{resampled}\right)}{Q_{resampled}} \times 100\%$$

where $Q_{original}$ is the peak discharge obtained using the original temporal pattern timestep and $Q_{resampled}$ is the peak obtained after rainfall resampling. Negative values indicate that the original timestep underestimates peak flow, while positive values indicate overestimation.

Case 2a: extreme hydrology study in a regional catchment

Case 2a examines an extreme hydrology assessment in a regional catchment in Victoria (Figure 3). The RORB model was delineated to relatively uniform subareas of approximately 4.5 km^2 (minimum 3.5 km^2, maximum 5.5 km^2). The outlet is a reservoir, and the dam inflow hydrograph is the output of interest.

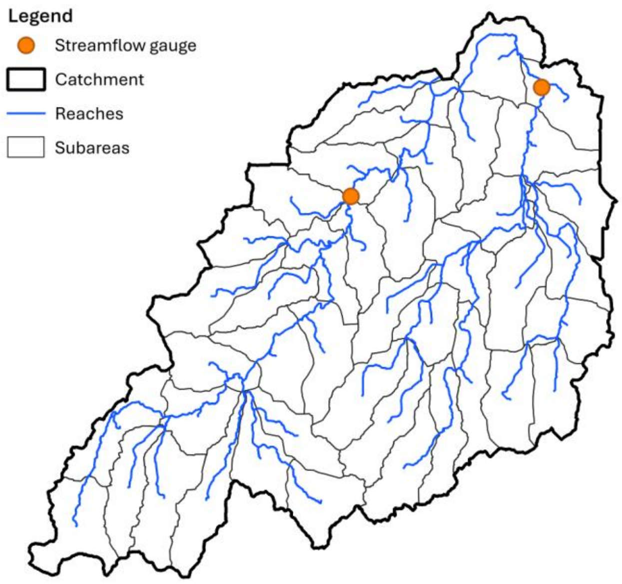

Figure 3 RORB layout of case 2a

The original k_c and m parameters from the design studies were adopted, while initial loss and continuing loss were set to zero. The model was calibrated to two upstream gauges using 6-minute pluviograph data, which therefore represents the timestep consistent with the calibrated catchment response.

Flood frequency changes

Resampling the design rainfall to a 6-minute timestep results in systematic changes to both peak flow and critical storm duration (Table 2). Peak flows are generally underestimated when the original timestep is used, with differences typically in the order of 1–5%. In addition, the governing storm duration shifts from 12 hours to 9 hours for events from 1 in 1,000,000 AEP through to PMPF. Under the original timestep, the 9-hour peaks are suppressed sufficiently that the 12-hour storm appears falsely critical. These changes are consistent with the oscillatory behaviour described Section 2.3, where coarse timesteps reduce peak flows and distort the relative ranking of storm durations.

Table 2 Comparison of flood frequency curve using original and resampled timestep for Case 2a

AEP	Critical duration changes after resampling	% difference in peak flow estimation
1 in 100,000	12 hour	1.1%
1 in 200,000	12 hour	0.9%
1 in 500,000	12 hour	0.8%
1 in 1,000,000	12 hour → 9 hour	-0.2%
1 in 2,000,000	12 hour → 9 hour	-1.7%
PMPF	12 hour → 9 hour	-3.5%
PMF	12 hour → 6 hour	-4.6%

Variation across storm durations

Peak flow differences vary significantly with storm duration (Table 3). The largest discrepancies occur for durations associated with coarse temporal patterns, particularly the 24-hour and 36-hour storms.

These durations exhibit differences of up to approximately 4–5%, while shorter durations with finer timesteps show smaller and more variable differences. Coarser temporal patterns introduce larger inflow changes between steps, which increases numerical distortion in the routed hydrograph.

Table 3 Percentage difference in peak flow estimation for each individual duration for Case 2a

AEP	3 hour ($\Delta t = 9$ min)	6 hour ($\Delta t = 15$ min)	9 hour ($\Delta t = 30$ min)	12 hour ($\Delta t = 30$ min)	24 hour ($\Delta t = 3$ hour)	36 hour ($\Delta t = 3$ hour)
1 in 100,000	-0.7%	0.2%	-2.5%	1.1%	-4.4%	-4.8%
1 in 200,000	-0.8%	0.1%	-2.8%	0.9%	-4.1%	-4.1%
1 in 500,000	-0.6%	-0.8%	-2.5%	0.8%	-4.4%	-2.1%
1 in 1,000,000	0.0%	-1.6%	-2.7%	0.6%	-4.9%	-2.0%
1 in 2,000,000	-0.2%	-1.6%	-3.0%	0.4%	-4.5%	-1.9%
PMPF	-0.2%	-1.4%	-3.5%	0.3%	-4.6%	-3.6%

Influence of temporal patterns

Results averaged across temporal patterns mask substantial variability at the individual pattern level. For the PMPF at 24-hour duration, peak-flow differences range from −15% to +2% (Table 4).

Table 4 Percentage difference in peak flow estimation for different temporal patterns for Case 2a

TP	% difference on peak flow	TP	% difference on peak flow	TP	% difference on peak flow	TP	% difference on peak flow
1	-2.3%	6	-3.3%	11	-4.9%	16	-2.5%
2	1.8%	7	-2.4%	12	-0.3%	17	-3.8%
3	-0.7%	8	-14.9%	13	-9.0%	18	0.2%
4	1.8%	9	-15.2%	14	-2.8%	19	-1.2%
5	-2.9%	10	-7.9%	15	1.5%	20	-6.5%

Several temporal patterns, particularly Patterns 8 and 9, show reductions exceeding 10% when the original timestep is used (Figure 4). These patterns are characterised by concentrated rainfall bursts or uneven distributions during the rising limb. In contrast, patterns with smoother rainfall distributions show smaller differences. The variability in both magnitude and sign reflects sensitivity to the timing and rate of inflow change, as described in Section 2.3.

Importantly, the 6-minute timestep corresponds to the timestep used during model calibration. Using the original coarser temporal-pattern timestep therefore means the model no longer represent the rainfall–runoff behaviour it was calibrated to.

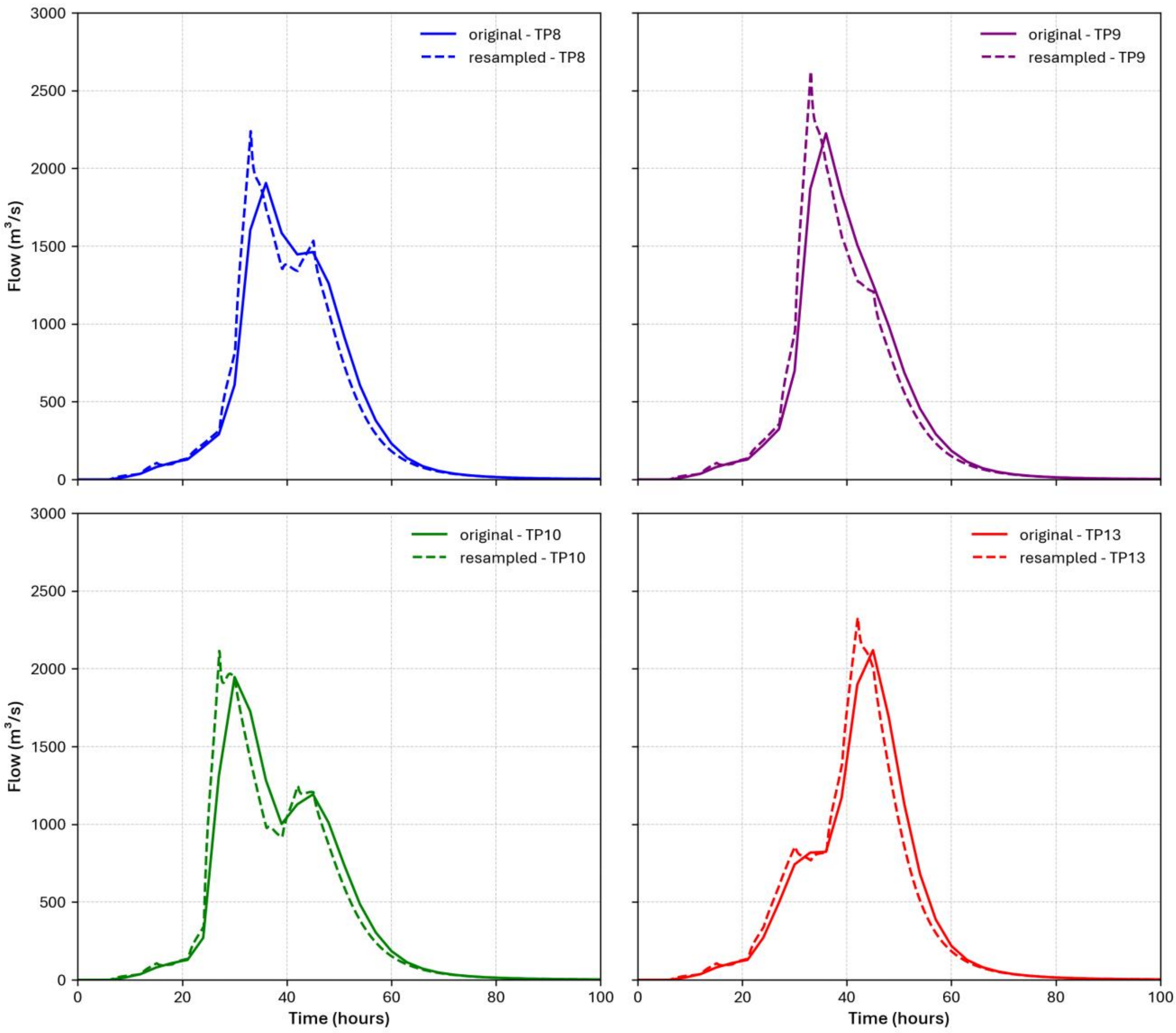

Figure 4 Comparison of original and resampled hydrographs for selected temporal patterns for Case 2a

Case 2b: general hydrology in 30 urban catchments

Case 2b examines the prevalence of instability across 30 urban catchments, focusing on the 1 in 100 AEP event. The design temporal patterns supplied by ARR DataHub was resampled to 1 minute. The original k_c and m parameters from the design studies were adopted, while initial loss and continuing loss were set to zero.

Mass-balance discrepancies

To identify instability within the routing network, a mass-balance comparison was performed for every reach. A reach was classified as having a mass-balance issue if the hydrograph volume difference between its upstream and downstream locations exceeded 10 % for any AEP–duration combination.

Figure 5 summarises the proportion of reaches affected across the 30 catchments. Instability is widespread:

- Only one catchment had less than 10 % of reaches affected.
- The majority of models had 20–40 % of reaches exhibiting mass-balance discrepancies.
- Several models had more than 40 % of reaches affected.

This confirms that oscillatory behaviour in RORB routing is not confined to isolated model configurations but can occur across a wide range of practical applications.

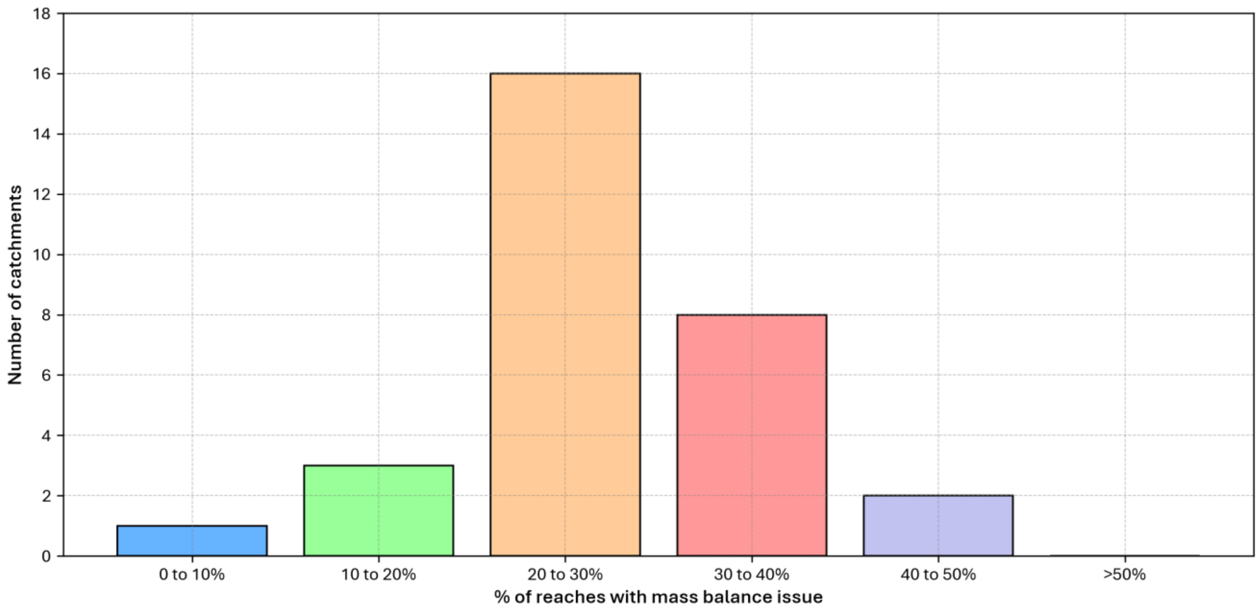

Figure 5 Reach mass balance summary for 30 urban catchment RORB models (Case 2b)

Peak-flow changes along reaches

Figure 6 summarises the percentage change along the most affected reach across the 30 urban catchments, while Table 5 presents the detailed results, including peak-flow differences and changes in critical storm duration. The reported values correspond to design flow estimates derived from the ensemble-based critical duration analysis.

Approximately one-third of catchments exhibit stable routing behaviour, with peak-flow differences within ±1%. In contrast, around half of the catchments show systematic peak-flow underestimation of 8–11% when the original timestep is used. In many of these cases, the critical storm duration also shifts following temporal resampling, indicating that oscillatory damping had previously suppressed peaks associated with shorter-duration storms.

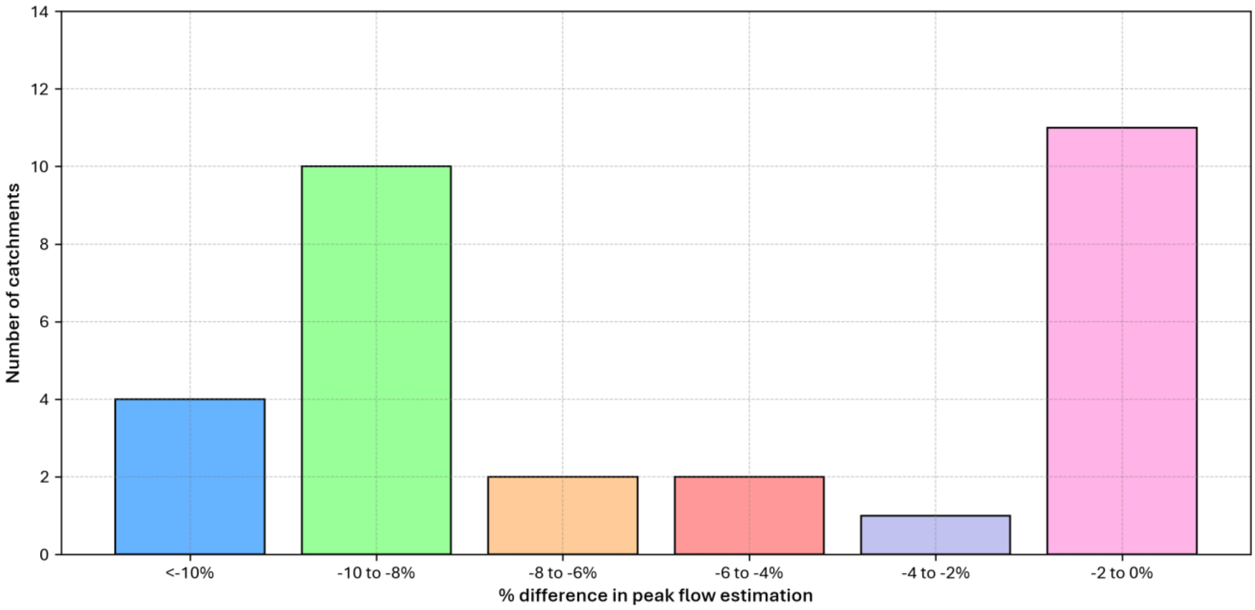

Figure 6 Percentage difference in peak flow estimation on the worst reach for 30 urban catchment RORB models (Case 2b)

Table 5 Percentage difference in peak flow estimation and critical duration change on the worst reach for 30 urban catchment RORB models

ID	Critical duration changes after resampling	% difference in peak flow estimation	ID	Critical duration changes after resampling	% difference in peak flow estimation	ID	Critical duration changes after resampling	% difference in peak flow estimation
1	20min → 10min	-8.3%	11	2 hour	-0.6%	21	10min	-9.0%
2	15min → 10min	-10.1%	12	15min → 10min	-9.6%	22	15min → 10min	-9.9%
3	15min → 10min	-9.7%	13	1 hour	-0.4%	23	10min	-3.1%
4	20min	-0.5%	14	15min → 10min	-9.4%	24	30min	-1.4%
5	1.5 hour	-0.1%	15	10min	-10.6%	25	15min → 10min	-10.1%
6	1 hour	-0.3%	16	15min → 10min	-8.2%	26	1.5 hour	-0.2%
7	10min	-5.3%	17	15min → 10min	-7.9%	27	10min	-5.6%
8	1.5 hour	-0.2%	18	30min	-1.4%	28	15min → 10min	-9.6%
9	15min	-9.3%	19	15min → 10min	-9.7%	29	1.5 hour	-0.5%
10	10min	-10.1%	20	15min → 10min	-6.4%	30	10min	-0.2%

Distortion of temporal patterns

A common industry practice in flood studies is to use the routed hydrograph from RORB as input to a hydraulic model. Unlike Case 2a, where RORB is treated as a lumped catchment model, intermediate hydrographs at internal reaches or print points are used as hydraulic model boundaries.

Figure 7 compares the original and resampled hydrographs for four representative hydrographs under Case 2b. The temporal pattern is noticeably distorted, particularly in the second example (purple), where a double-peaked event is transformed into a single peak. Across all cases, the resampled hydrographs exhibit earlier and sharper peaks, with a shortened rising limb and a more attenuated recession. These results show that temporal resampling alters not only peak flow but also the distribution of flow over time, effectively redistributing volume within the event and modifying the hydrograph shape in a way that may influence downstream hydraulic response.

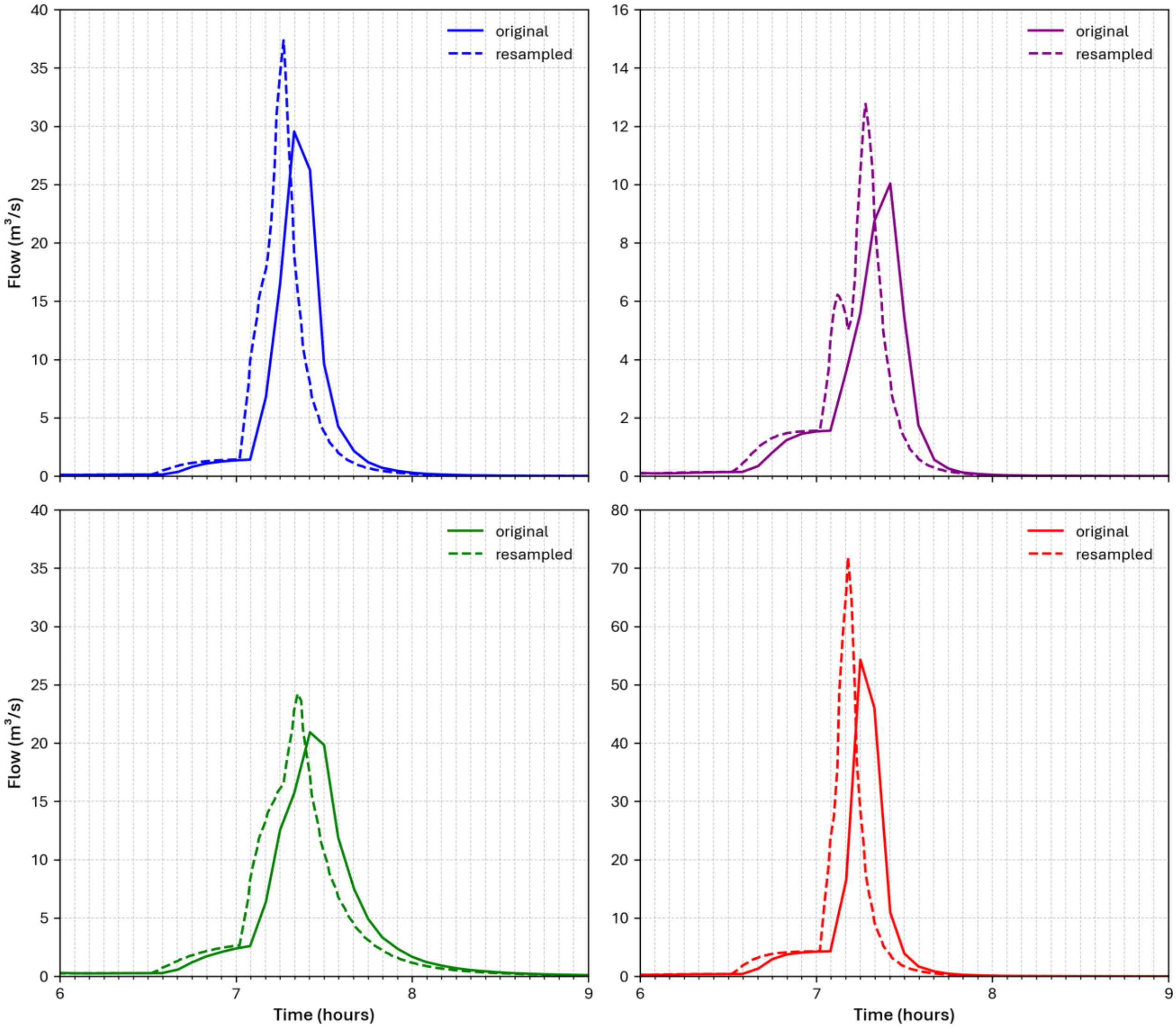

Figure 7 Comparison of original and resampled hydrographs for representative hydrographs under Case 2b

Discussion

While oscillatory artefacts in RORB can be significant, their influence on model results is case dependent. Additional testing on a separate dam catchment in Queensland, similar in scope to Case 2a, showed minimal instability. This catchment exhibited a slower hydrological response, such that the timestep remained small relative to the catchment response time. Under these conditions, oscillatory behaviour was limited and had negligible impact on model outputs. In contrast, fast-response systems, as demonstrated in Case 2a, are more susceptible to instability due to their shorter response times and steeper hydrographs.

For Case 2b, the reported differences correspond to the most affected reach within each catchment. In practical applications, locations of interest are often further downstream, where routing through multiple reaches introduces attenuation. This process can reduce peak differences; however, it does not eliminate the underlying numerical artefacts. Instead, oscillations are partially damped and redistributed, meaning that apparent agreement in peak magnitude may mask distortions in hydrograph timing and shape.

These distortions are evident in Case 2b, where temporal resampling alters the hydrograph structure. Double-peaked events may be smoothed into a single peak, while peaks can shift earlier and become sharper, with a shortened rising limb and a more attenuated recession. Although total event volumes may appear comparable, the internal redistribution of flow can be substantial. Such effects are not always apparent when assessment is limited to peak discharge or outlet hydrographs.

This has direct implications for hydraulic modelling workflows, where routed hydrographs from RORB are commonly applied as boundary conditions in models such as TUFLOW. Under these conditions, distortions in hydrograph shape, including peak suppression, timing shifts, and volume inconsistencies, directly affect the hydraulic response. Impacts are most pronounced in urban and rapidly responding catchments, where flood behaviour is sensitive to both flow magnitude and timing. In these systems, even moderate oscillatory artefacts can influence peak water levels, inundation timing, and predicted flood extents.

A further key finding is that instability depends not only on timestep, but also on flow magnitude. As flows increase, the storage–discharge relationship becomes flatter (i.e. $\frac{dS}{dQ}$ decreases), reducing the effective damping of the system. This increases the relative timestep size compared to the system response time, making oscillatory behaviour more likely. Consequently, a timestep that appears adequate under calibration conditions may still produce instability during extreme event simulations. This behaviour is evident in Case 2a, where instability becomes more pronounced under design events, leading to suppression of peak flows and shifts in critical storm duration.

Mass balance discrepancies are intrinsically linked to this oscillatory behaviour. As demonstrated in Case 2b, inconsistencies arise across reaches when hydrographs are examined throughout the routing network, and similar effects would be expected in Case 2a. This compromises volume consistency, which is critical for applications involving detention performance, floodplain storage, and cumulative downstream impacts.

Overall, these findings demonstrate that timestep selection is not purely a numerical consideration, but a key modelling decision. While instability may be negligible in slower catchments or when only outlet flows are of interest, it can become material in fast-response systems and under extreme conditions. Careful alignment between timestep, catchment response, and modelling objectives is therefore required to produce physically consistent results.

4. Stabilising RORB using the hydrological Courant number

The analytical results presented earlier suggest that instability is governed by the relationship between timestep and storage response time. In hydraulic models, the Courant number constrains the timestep so that numerical updates do not outrun the physical propagation of information. An analogous stability condition can be defined for RORB routing to characterise when oscillatory behaviour occurs.

From the oscillation criterion derived in Section 3, oscillatory artefacts are avoided when:

$$\Delta t \leq 2\lambda_t \tag{29}$$

where λ_t represents the effective storage timescale:

$$\lambda_t = \frac{dS}{dQ} = 3600kmQ_t{}^{m-1} \tag{30}$$

In RORB (RORB Manual, 2010), the storage parameter k_i is defined as:

$$k_i = k_c \times k_{r,i}, \qquad k_{r,i} = F_i \times \frac{L_i}{d_{av}} \tag{31}$$

where k_c is the global routing parameter, L_i is the reach length, d_{av} is the average flow distance across the catchment, and F_i is a reach-type factor (typically 1.0 for natural channels).

Substituting into Equation (30) gives:

$$\lambda_t = 3600k_c\left(F_i\frac{L_i}{d_{av}}\right)mQ_{i,t}^{m-1} \tag{32}$$

The non-oscillation timestep criterion therefore becomes:

$$\Delta t \leq 7200k_c\left(F_i\frac{L_i}{d_{av}}\right)mQ_{i,t}^{m-1} \tag{33}$$

This expression can be interpreted as a hydrological Courant condition, where the timestep is constrained by the ratio between numerical resolution and the effective travel time of the storage element.

Several key implications follow:

- The allowable timestep increases with calibration parameter k_c, as larger values represent greater storage inertia.
- The allowable timestep increases with reach length L_i, meaning longer reaches are less sensitive to timestep effects.
- For $m < 1$, the allowable timestep decreases with increasing flow, making high-flow conditions the most restrictive.
- Stability is not a fixed property of the model, but varies throughout the hydrograph and is the most restrictive at peak flow, where instability is most likely to be triggered.

5. Recommendations for modellers

The following recommendations summarise practical implications for model setup and application.

More subareas do not necessarily improve results.

A finer subarea discretisation does not guarantee improved physical representation. Reducing subarea size shortens reach lengths and reduces travel time, and therefore reduces storage effects and increases responsiveness. If the timestep is not reduced accordingly, the ratio between timestep and response time increases, making the routing more prone to oscillatory behaviour. In such cases, increasing model resolution can degrade numerical behaviour rather than improve it.

Consistent reach length is important.

Large variations in reach length within a model can lead to inconsistent routing behaviour. Short reaches are more sensitive to timestep effects and are more likely to exhibit oscillatory artefacts. Maintaining a consistent range of reach lengths helps produce more uniform routing behaviour and reduces the likelihood of localised instability within the network.

Design timestep should be consistent with calibration conditions.

Model calibration implicitly defines a timestep that is consistent with the catchment response. Applying coarser timesteps in design simulations alters the numerical behaviour of the routing scheme, even if model parameters remain unchanged.
To maintain consistency between calibration and application, the design timestep should be aligned with the timestep used during calibration, particularly for fast-response catchments.

Use a consistent timestep across all storm durations.

Design temporal-pattern datasets often use different timesteps for different durations. Longer durations are commonly associated with coarser timesteps, which increases susceptibility to oscillatory behaviour. Using inconsistent timesteps across durations can introduce artificial bias in peak flow estimation and critical duration selection. A consistent rainfall timestep should therefore be applied across all durations to maintain comparability.

Evaluate stability under design flow conditions, not only calibration events.

Routing stability depends not only on timestep, but also on flow magnitude. A timestep that performs adequately under calibration conditions may therefore become unstable under extreme design events. Stability checks should be carried out under peak design flow conditions, not just historical events.

Exercise caution when using routed flows as hydraulic model inputs.

When routed hydrographs are used as boundary conditions for hydraulic models, any numerical artefacts are transferred directly into downstream simulations. This includes peak suppression, timing distortion, and mass-balance inconsistencies. The risk is greatest in urban and fast-response systems, where hydraulic results are sensitive to both peak flow and volume. Particular care should be taken where short reaches are used, as these are more prone to instability and can introduce localised errors that propagate downstream.

6. Conclusion

This study has demonstrated that oscillatory numerical artefacts in RORB routing arise from the time discretisation of the storage equation and are governed by the relationship between timestep and the effective storage response time. While the underlying formulation has remained unchanged since the model's development, contemporary modelling practices have evolved significantly, with increasingly fine spatial discretisation and widespread use of routed hydrographs in downstream hydraulic modelling. This shift has increased the likelihood that routing instability can occur in practical applications.

The results show that these artefacts are not confined to theoretical cases but can manifest in real-world models, particularly in short reaches, high-flow conditions, and fast-response catchments. Their effects include peak-flow suppression, shifts in critical storm duration, temporal pattern distortion, and mass-balance inconsistencies, all of which can influence flood estimates and hydraulic modelling outcomes.

Importantly, these instabilities are not readily detectable using standard modelling workflows and can remain hidden while still affecting results. This highlights a gap between current modelling practice and the numerical behaviour of the routing scheme, which has received limited attention despite increasing model complexity.

The findings lead to several practical recommendations. Model discretisation should be undertaken with consideration of reach length consistency rather than maximising spatial resolution. The timestep applied in design simulations should be consistent with calibration conditions and maintained across all storm durations. Stability should be assessed under peak design flows, not only historical events, and particular caution is required when routed hydrographs are used as inputs to hydraulic models. Short reaches should be avoided or carefully assessed, as they are more susceptible to instability.

The proposed hydrological Courant condition provides a simple and physically interpretable framework to relate timestep, reach length, and flow conditions. It offers a practical screening tool to identify configurations that are likely to produce unstable routing behaviour.

Overall, this work highlights that timestep selection and catchment discretisation are not independent modelling choices, but fundamental controls on model reliability. As flood modelling continues to adopt higher-resolution data and more complex configurations, greater attention to these aspects is required to produce physically consistent and defensible results in hydrology assessments using RORB.

References

RORB Manual (2010), *RORB Version 6 Runoff Routing Program User Manual*.